




REPORT

# IPO11 mediates $\beta$ catenin nuclear import in a subset of colorectal cancers

Monika Mis<sup>1</sup>, Siobhan O'Brien<sup>2</sup>, Zachary Steinhart<sup>1</sup>, Sichun Lin<sup>1</sup>, Traver Hart<sup>3,4</sup> , Jason Moffat<sup>4,5,6</sup> , and Stephane Angers<sup>1,2</sup> 

**Activation of Wnt signaling entails  $\beta$ catenin protein stabilization and translocation to the nucleus to regulate context-specific transcriptional programs. The majority of colorectal cancers (CRCs) initiate following APC mutations, resulting in Wnt ligand-independent stabilization and nuclear accumulation of  $\beta$ catenin. The mechanisms underlying  $\beta$ catenin nucleocytoplasmic shuttling remain incompletely defined. Using a novel, positive selection, functional genomic strategy, DEADPOOL, we performed a genome-wide CRISPR screen and identified *IPO11* as a required factor for  $\beta$ catenin-mediated transcription in APC mutant CRC cells. *IPO11* (Importin-11) is a nuclear import protein that shuttles cargo from the cytoplasm to the nucleus. *IPO11*<sup>-/-</sup> cells exhibit reduced nuclear  $\beta$ catenin protein levels and decreased  $\beta$ catenin target gene activation, suggesting *IPO11* facilitates  $\beta$ catenin nuclear import. *IPO11* knockout decreased colony formation of CRC cell lines and decreased proliferation of patient-derived CRC organoids. Our findings uncover a novel nuclear import mechanism for  $\beta$ catenin in cells with high Wnt activity.**

## Introduction

During embryonic development and adult tissue homeostasis, the Wnt- $\beta$ catenin signaling pathway governs context-dependent transcriptional programs regulating stem cell renewal, cell proliferation, and differentiation (Wodarz and Nusse, 1998; Steinhart and Angers, 2018). In the absence of Wnt ligand, the destruction complex composed of APC, Axin, GSK3 $\alpha/\beta$ , and CK1 $\alpha$  earmarks  $\beta$ catenin for proteasomal degradation (Dominguez et al., 1995; Marikawa and Elinson, 1998; Behrens et al., 1998; Peters et al., 1999). Activation of the pathway by Wnt stabilizes  $\beta$ catenin, where it translocates into the nucleus to promote transcription of context-dependent target genes (Angers and Moon, 2009; Cadigan and Waterman, 2012).

Aberrant activation of Wnt- $\beta$ catenin signaling is a driver of colorectal cancer (CRC) initiation. APC loss-of-function mutations occur in 80% of CRCs (Cancer Genome Atlas Network, 2012) and inactivate the destruction complex, leading to stabilization and nuclear accumulation of  $\beta$ catenin (Morin et al., 1997). Subsequent mutations in *KRAS*, *TP53*, and *SMAD4* further promote tumor progression into carcinoma (Fearon, 2011; Fearon and Vogelstein, 1990); however,  $\beta$ catenin signaling is still required for advanced tumor maintenance (Scholer-Dahirel et al., 2011; Dow et al., 2015). Despite this, there are

no clinically approved therapeutics to target the Wnt- $\beta$ catenin pathway.

The nuclear localization of  $\beta$ catenin is controlled by its rate of nuclear entry versus exit, along with retention factors anchoring  $\beta$ catenin in the cytoplasm or nucleus. Pygo/Pygopus constitutively localizes to the nucleus and recruits Lgs/BCL9, which binds  $\beta$ catenin to promote its nuclear localization (Townesley et al., 2004). TCF7L2/TCF4 acts similarly, binding  $\beta$ catenin in the nucleus, leading to increased nuclear retention, whereas in the cytoplasm,  $\beta$ catenin is bound by APC and Axin, preventing  $\beta$ catenin nuclear localization (Krieghoff et al., 2006). Normally, APC continuously shuttles in and out of the nucleus. Mutations in APC in CRC remove its nuclear export signal, resulting in nuclear accumulation and promotion of  $\beta$ catenin nuclear retention (Henderson, 2000; Rosin-Arbesfeld et al., 2003).

The molecular mechanisms underlying  $\beta$ catenin nuclear transport remain unclear (Jamieson et al., 2014). Proteins with a nuclear localization signal (NLS) are recognized by Importin- $\alpha$  proteins, a scaffold for Ran-binding Importin- $\beta$  proteins (Rexach and Blobel, 1995). The directionality of cargo transport is regulated by the Ran-GTP gradient. It is thought that  $\beta$ catenin binds the nuclear pore complex directly via its armadillo repeats,

<sup>1</sup>Department of Pharmaceutical Sciences, Leslie Dan Faculty of Pharmacy, University of Toronto, Toronto, Ontario, Canada; <sup>2</sup>Department of Biochemistry, University of Toronto, Toronto, Ontario, Canada; <sup>3</sup>Department of Bioinformatics and Computational Biology, MD Anderson Cancer Center, Houston, TX; <sup>4</sup>Donnelly Centre, University of Toronto, Toronto, Ontario, Canada; <sup>5</sup>Department of Molecular Genetics, University of Toronto, Toronto, Ontario, Canada; <sup>6</sup>Canadian Institute for Advanced Research, Toronto, Ontario, Canada.

Correspondence to Stephane Angers: [stephane.angers@utoronto.ca](mailto:stephane.angers@utoronto.ca).

© 2019 Mis et al. This article is distributed under the terms of an Attribution-Noncommercial-Share Alike-No Mirror Sites license for the first six months after the publication date (see <http://www.rupress.org/terms/>). After six months it is available under a Creative Commons License (Attribution-Noncommercial-Share Alike 4.0 International license, as described at <https://creativecommons.org/licenses/by-nc-sa/4.0/>).

which share homology with Importin- $\alpha$  and Importin- $\beta$ . However,  $\beta$ catenin does not associate with the same nuclear pore proteins that Importin- $\beta$ 1 (also known as KPNB1) utilizes for transport (Suh and Gumbiner, 2003), does not contain a classical NLS, nor does it bind Importin- $\beta$ 1 in vitro (Yokoya et al., 1999). The role of Ran in  $\beta$ catenin nuclear import is still up for debate. Although  $\beta$ catenin lacks a Ran-binding domain, its transport is inhibited by a nonhydrolyzable GTP analog or a dominant-negative Ran mutant (Fagotto et al., 1998). A conflicting study reported that  $\beta$ catenin nuclear localization was independent of the Ran gradient (Yokoya et al., 1999). These inconsistencies point toward uncharacterized mechanisms of  $\beta$ catenin transport, where additional factors may mediate  $\beta$ catenin nuclear localization in parallel, or to different mechanisms that are context dependent. Nucleocytoplasmic trafficking mediated by Importin- $\beta$  carrier proteins is necessary for a variety of cellular functions. The Importin- $\beta$  family comprises 11 protein-coding genes in humans (*KPNB1*, *IPO4*, *IPO5*, *IPO7*, *IPO8*, *IPO9*, *IPO11*, *IPO13*, *TNPO1*, *TNPO2*, and *TNPO3*), and each has its own biological roles and transports unique sets of cargo (Kimura et al., 2017; Mackmull et al., 2017; Kimura and Imamoto, 2014).

CRISPR-Cas9 technologies have enabled forward genetic screens in cultured cells with unprecedented sensitivity and specificity (Shalem et al., 2014; Hart et al., 2015). Given that signal transduction mechanisms of  $\beta$ catenin downstream of the destruction complex are poorly understood and the potential clinical implications for CRC, we aimed to identify genes required for constitutive  $\beta$ catenin transcriptional activity in CRC cells harboring *APC* mutations. We developed a reporter-based positive-selection screening strategy and used CRISPR-Cas9-mediated gene editing to perform genetic suppressor screens to identify genes required for  $\beta$ catenin signal transduction in *APC* mutant CRC cells. Notably, we identified *IPO11*, which encodes the Importin- $\beta$  family protein IPO11 (Importin-11), which is known to shuttle cargo from the cytoplasm to the nucleus in a Ran-dependent manner (Plafker and Macara, 2000). We demonstrated the requirement of *IPO11* for  $\beta$ catenin nuclear transport and transcriptional activity, furthering our understanding of distal  $\beta$ catenin signaling in a CRC context.

## Results and discussion

### Development of DEADPOOL, a CRISPR screening platform for identification of genes required for signaling systems

To identify genes required for intracellular signaling events, we used an inducible suicide gene reporter as a positive selection system for pooled lentiviral CRISPR-Cas9 screens, designated DEADPOOL. We engineered the DLD-1 CRC cell line (which contains a frameshift mutation causing an *APC* truncation at position 1417) to express  $\beta$ catenin-dependent LEF-TCF DNA-binding elements directing the expression of an inducible form of the apoptosis-inducing protease Caspase-9 (iCasp9; Straathof et al., 2005; Di Stasi et al., 2011). In iCasp9, the dimerization domain of Caspase-9 was replaced with the FKBP (F36V) domain that dimerizes in the presence of small molecule AP20187 (Fig. 1 A, "AP"). Constitutive nuclear  $\beta$ catenin signaling in DLD-1 cells led to iCasp9 protein expression without toxicity

until the addition of AP20187, causing cell death (Fig. 1, A and B). DLD-1  $\beta$ catenin-DEADPOOL cells were further engineered to express Cas9 to enable gene editing. Cells that survive the lethal dose of AP20187 were predicted to harbor loss-of-function mutations within genes essential for  $\beta$ catenin-mediated transcriptional activity in this context (Fig. 1 C). Validating the system, cells infected with two independent gRNA targeting *CTNNB1*, which encodes  $\beta$ catenin, were resistant to induction of cell death triggered by AP20187 (Fig. 1 D). The DEADPOOL platform constitutes a robust system to conduct genetic suppressor screens for the identification of genes involved in signaling systems.

### *IPO11* is required for $\beta$ catenin-dependent signaling in CRC cells

We performed a genome-wide  $\beta$ catenin-DEADPOOL CRISPR screen to identify genes required for  $\beta$ catenin-mediated transcriptional activity in the context of CRC harboring *APC* mutations (Figs. 1 C and 2 A). Strikingly, only eight genes with at least three gRNA with an enrichment Z score  $>3$  were identified. Among these,  $\beta$ catenin (*CTNNB1*) and its known cotranscriptional activator *BCL9L* (Kramps et al., 2002) were the top- and third-ranked genes in the screen, respectively (Fig. 2, A and B). The second-highest ranked gene was *IPO11*, a gene with no previous link to  $\beta$ catenin-mediated signaling (Fig. 2, A and B). Validating the screen results, DLD-1  $\beta$ catenin-DEADPOOL cells infected with two independent gRNA targeting *IPO11* were resistant to 1 nM AP20187 (Fig. 2 C). Overexpression of FLAG-*IPO11* using cDNA resistant to *IPO11* #1 and #2 gRNAs resensitized the reporter to 1 nM AP20187 (Fig. 2 C). Knockout (KO) of *IPO11* reduced the activity of the pBAR  $\beta$ catenin-dependent luciferase reporter, confirming that *IPO11* is required for  $\beta$ catenin-mediated transcription and not direct iCasp9 activity (Fig. 2 D). Expression of several  $\beta$ catenin-dependent target genes previously found to be induced in CRC lines (Major et al., 2008) was also inhibited in *IPO11*<sup>-/-</sup> cells (Fig. S1, B and C), confirming that the function of *IPO11* is not limited to synthetic transcriptional reporters (Fig. 2 E). Overexpression of LEF1-VP16, which induces expression of TCF/LEF target genes independent of  $\beta$ catenin, resensitized DLD-1  $\beta$ catenin-DEADPOOL cells infected with *IPO11* gRNA to iCasp9-mediated cell death, suggesting that *IPO11* functions upstream or at the level of  $\beta$ catenin (Fig. 2 F). This indicates that *IPO11* is required for expression of the  $\beta$ catenin transcriptional program in DLD-1 CRC cells.

### *IPO11* is required for $\beta$ catenin nuclear import in *APC* mutated CRC cells

We next set out to determine the mechanism underlying *IPO11* action in the  $\beta$ catenin signaling pathway. Compared with control, DLD-1 *IPO11*<sup>-/-</sup> cells showed reduction in nuclear  $\beta$ catenin protein (Fig. 3 A). In support, CRISPR-Cas9-mediated targeting of *IPO11* in SW480 cells, another *APC* mutated CRC cell line, strongly inhibited the nuclear localization of  $\beta$ catenin as detected by immunofluorescence (Fig. 3 B). Subcellular fractionation of HCT116 CRC cells containing an activating Ser45 mutation of  $\beta$ catenin revealed that gRNA targeting of *IPO11* had marginal effect on nuclear  $\beta$ catenin in this context (Fig. 3 C). A similar observation was made in RKO CRC cells, which

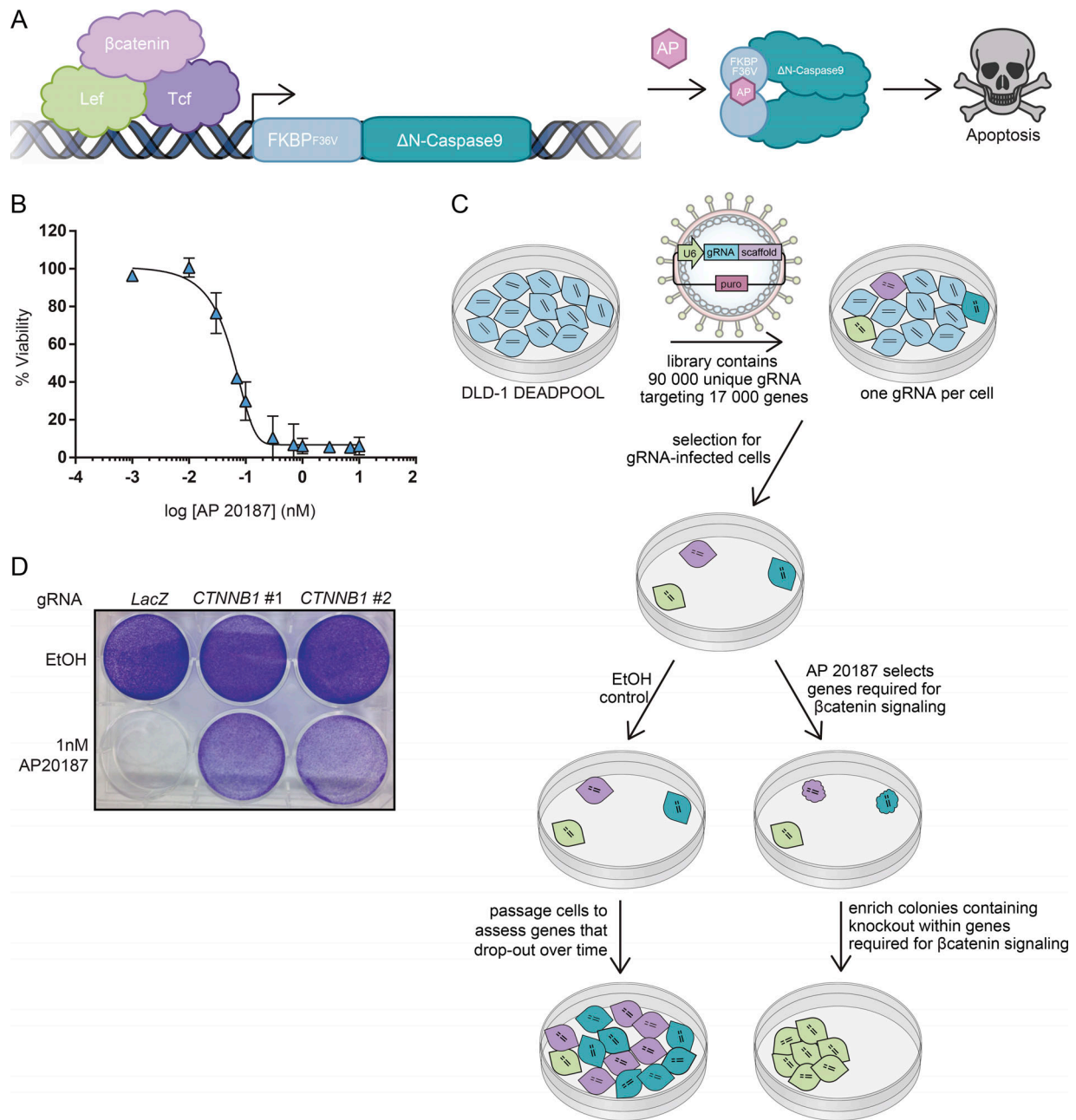


Figure 1. **Development and validation of DLD-1  $\beta$ catenin-DEADPOOL cells.** (A) Schematic of the  $\beta$ catenin-dependent iCasp9 system. (B) AP20187 (AP) dose-response curve in DLD-1  $\beta$ catenin-DEADPOOL cells. Mean  $\pm$  SD,  $n = 3$  independent experiments. (C) Schematic of genome-wide suppressor screen to identify genes required for  $\beta$ catenin signaling in CRC. (D) Crystal violet stain of DLD-1 iCasp9/Cas9 line transduced with lentiviral vectors enabling expression of LacZ, CTNNB1 #1, or CTNNB1 #2 gRNA and treated with EtOH or 1 nM AP20187. Representative of three independent experiments.

do not harbor mutations within Wnt signaling components. Stimulation of RKO cells with WNT3A led to nuclear accumulation of  $\beta$ catenin in both control and *IPO11*<sup>-/-</sup> RKO cells (Fig. 3 D). Furthermore, when we analyzed publicly available genome-wide CRISPR-Cas9 fitness screen data from CRC cell lines, we found the presence of APC mutation to be positively correlated with dependency on *IPO11* for fitness (Fig. 3 E). These data suggest that *IPO11* is required for  $\beta$ catenin nuclear accumulation and signaling selectively in CRC cells harboring APC mutations.

#### IPO11 binds to $\beta$ catenin and mediates its nuclear import

*IPO11* is known to directly interact with its cargos UBE2E3 and PTEN to mediate their nuclear transport (Plafker and Macara, 2000; Chen et al., 2017). Given that the observed decrease in nuclear  $\beta$ catenin levels in *IPO11*<sup>-/-</sup> CRC cells is not attributable to changes in  $\beta$ catenin mRNA levels (Fig. S1 A), we next determined whether *IPO11* participated in  $\beta$ catenin nucleocytoplasmic shuttling. First, using an in vitro binding assay, we observed that  $\beta$ catenin interacted directly with *IPO11* in a Ran-dependent manner (Fig. 4 A). Binding was confirmed in HEK293T cells

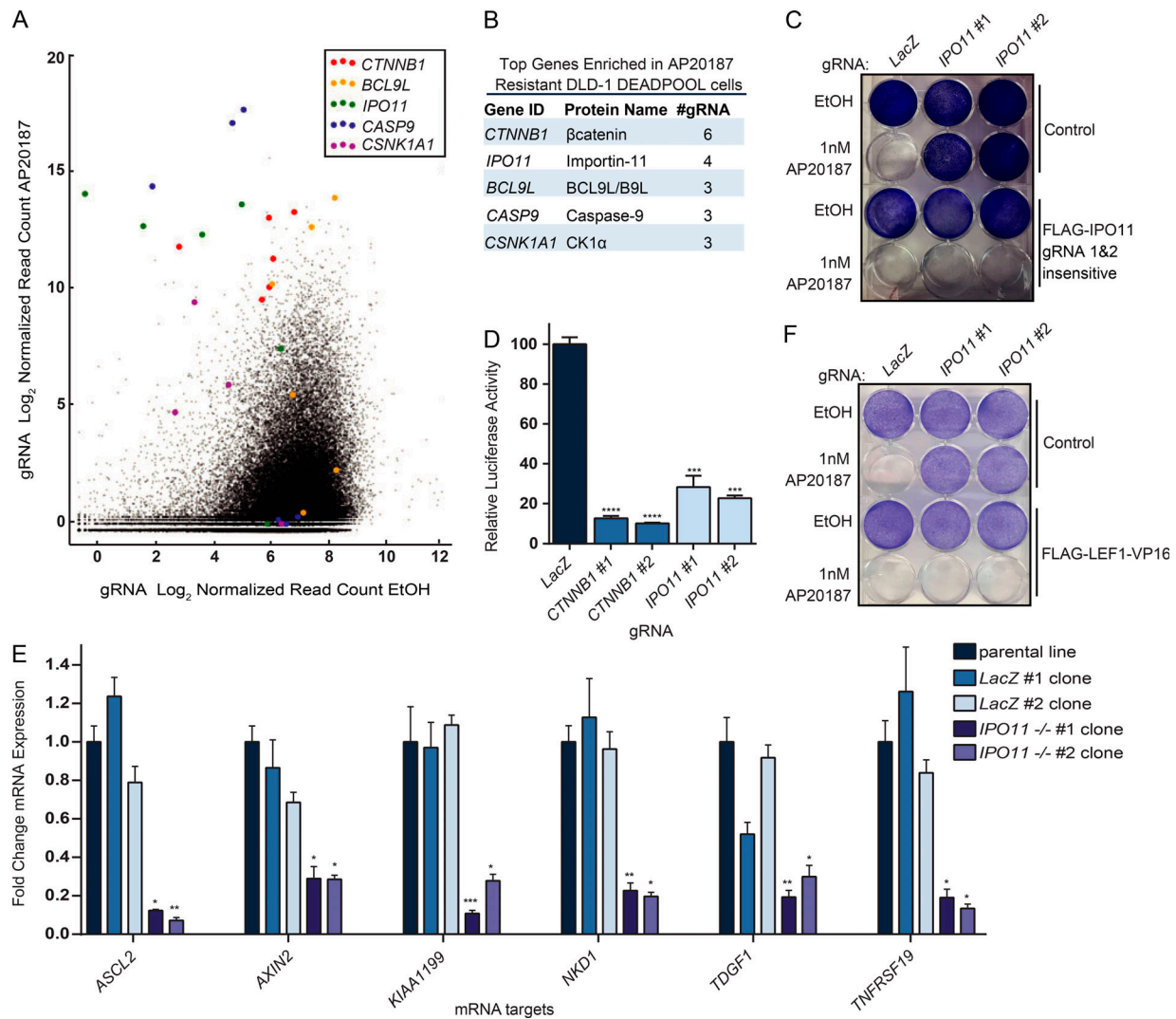
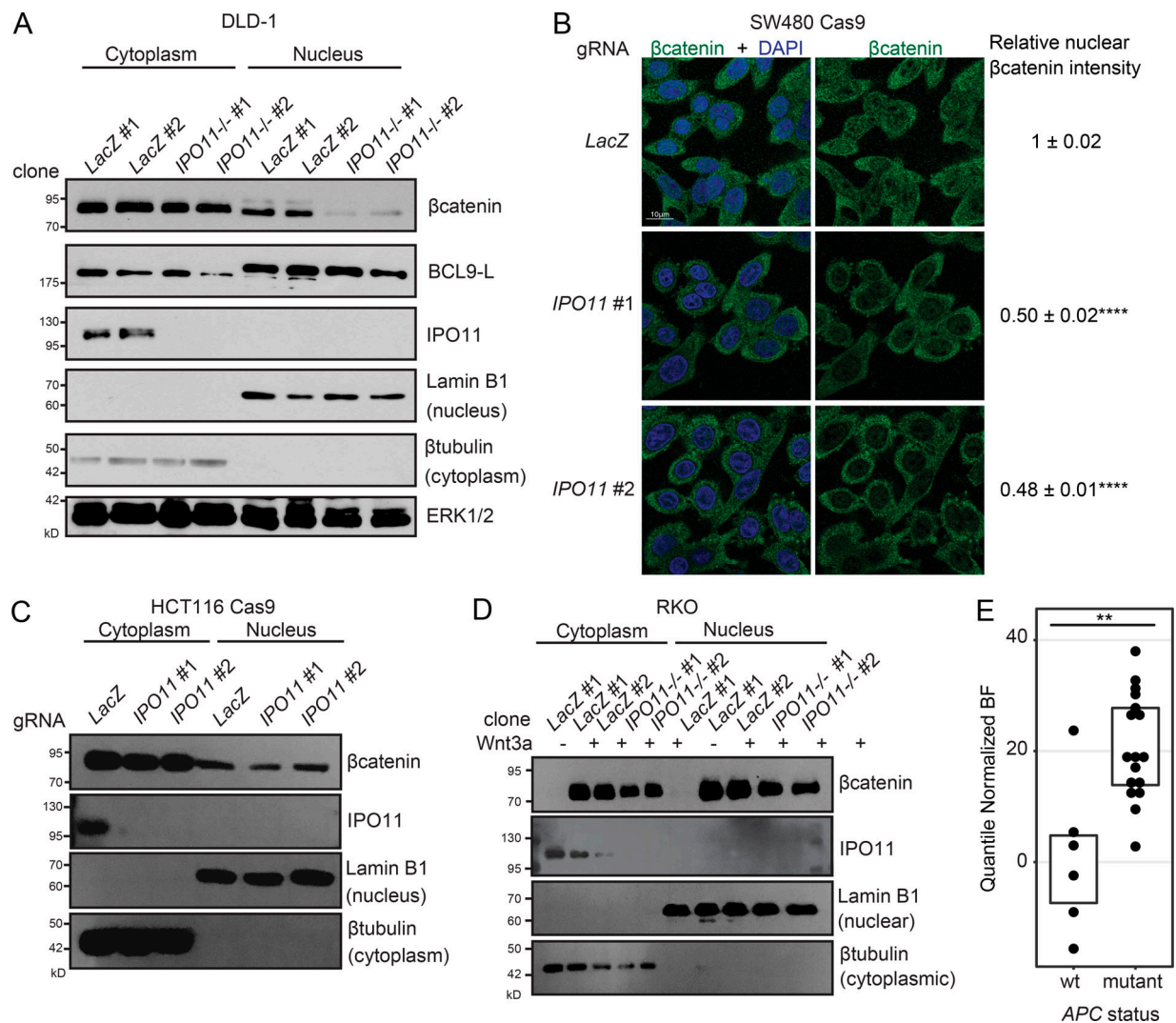


Figure 2. **Genome-wide CRISPR-Cas9 DEADPOOL screen identifies *IPO11* as a gene required for  $\beta$ catenin signaling.** (A) Scatter plot of normalized read counts for each gRNA in 1 nM AP20187 versus EtOH. (B) Top genes identified from the screen, ranked by the number of unique guides with a Z score >3. (C) Crystal violet stain of DLD-1  $\beta$ catenin-DEADPOOL cells expressing FLAG-IPO11 cDNA (*IPO11* gRNA #1 and #2 insensitive) expressing LacZ, *IPO11* #1, or *IPO11* #2 gRNA and treated with EtOH or 1 nM AP20187. (D) DLD-1 expressing Cas9, pBAR  $\beta$ catenin-dependent luciferase reporter, and LacZ, *IPO11* #1, and *IPO11* #2 gRNA.  $n = 3$  independent experiments. (E) RT-qPCR of  $\beta$ catenin target genes in monoclonal DLD-1 *IPO11* KO lines.  $n = 3$  independent experiments. (F) Crystal violet stain of DLD-1  $\beta$ catenin-DEADPOOL cells expressing FLAG-LEF1-VP16 and LacZ, *IPO11* #1, or *IPO11* #2 gRNA and treated with EtOH or 1 nM AP20187. Bars represent mean fold change  $\pm$  SD. Statistical analyses were performed by one-way ANOVA followed by Dunnett's multiple comparison test. \*,  $P \leq 0.05$ ; \*\*,  $P \leq 0.01$ ; \*\*\*,  $P \leq 0.001$ ; \*\*\*\*,  $P \leq 0.0001$ .

when overexpressed *IPO11*, but not Importin- $\beta$ 1, was coimmunoprecipitated with a constitutively active  $\beta$ catenin S $\rightarrow$ A (S33A/S37A/T41A/S45A) mutant (Fig. 4 B). Expression of a dominant-negative Ran mutant, Ran(Q69L), which constitutively binds GTP and disrupts Ran-dependent shuttling of cargo from the cytoplasm to the nucleus, inhibited the association of  $\beta$ catenin with *IPO11*, suggesting this nuclear import mechanism is Ran dependent (Fig. 4 B). Accordingly, expression of  $\Delta$ N-*IPO11*, which is a mutant predicted to be impaired in Ran binding, in the DLD-1  $\beta$ catenin-DEADPOOL cells rescued the AP20187-dependent killing (Fig. 4 C). We next set out to identify  $\beta$ catenin's structural domains underlying its *IPO11*-dependent nuclear localization. To do so, we fused full-length  $\beta$ catenin as well as three independent domains (N-terminal, armadillo

repeats, and C-terminal) to eGFP- $\beta$ galactosidase to allow visualization by microscopy and to sufficiently increase the molecular weight of these fusion proteins to prevent passive diffusion through the nuclear pores (Fig. 4 D and Fig. S2 C). Each domain (N-terminal, armadillo repeats, and C-terminal) localized to the nucleus of control cells, but nuclear localization of full-length  $\beta$ catenin and the isolated C-terminal domain was significantly decreased in *IPO11*<sup>-/-</sup> cells (Fig. 4, E and F). We conclude that determinants present on the C-terminus of  $\beta$ catenin are required for *IPO11*-mediated nuclear translocation.

To distinguish whether *IPO11* plays a role in active nuclear import or nuclear retention of  $\beta$ catenin, we tagged  $\beta$ catenin with a classical NLS to reroute its nuclear import through the



**Figure 3. IPO11 regulates nuclear βcatenin protein levels in APC mutant CRC cells.** (A) DLD-1 control and *IPO11*<sup>-/-</sup> cells fractionated into cytoplasmic and nuclear compartments and immunoblotted for the indicated proteins. Representative image of three independent experiments. (B) Immunofluorescence detection of βcatenin subcellular localization in SW480 Cas9 cells expressing *LacZ*, *IPO11* #1, and *IPO11* #2 gRNA. Quantification is mean intensity of fluorescence ± SD of three replicates. Statistical analysis was performed by one-way ANOVA Dunnett's test. \*\*\*\*, *P* < 0.0001. (C) HCT116 cells expressing *LacZ*, *IPO11* #1, and *IPO11* #2 gRNA were fractionated into cytoplasmic and nuclear compartments and immunoblotted for the indicated proteins. Representative image of three replicates. (D) RKO control and *IPO11*<sup>-/-</sup> cells were stimulated with WNT3A conditioned media, fractionated into cytoplasmic and nuclear compartments, and immunoblotted for the indicated proteins. Representative image of three independent experiments. (E) Dot plot of Bayes Factor (BF) for *IPO11* in *APC* wild-type (wt; *n* = 6) and *APC* mutated cell lines (*n* = 17). Mann-Whitney *U* test, \*\*, *P* < 0.001. Retrieved from PICKLES (Lenoir et al., 2018). BF > 5 represents high-confidence essential gene.

Importin-α/Importin-β1 complex. Since NLS-βcatenin localized properly to the nucleus in *IPO11*<sup>-/-</sup> DLD-1 cells (Fig. 4 G), *IPO11* does not play a role in the retention of βcatenin in the nucleus.

Finally, a nuclear import assay was performed using purified FITC-conjugated βcatenin and IPO11 in semi-permeabilized HeLa cells (Fig. S3, A and B). Although βcatenin alone, in the absence of nuclear import factors, is able to transit into the nucleus, the addition of recombinant IPO11 increased its nuclear localization (Fig. 4 H). The addition of dominant-negative Ran(Q69L) blocked the IPO11 effect and hence confirmed the requirement for Ran GTPase activity in this process. We conclude that IPO11 interacts with βcatenin and mediates its nuclear import in a Ran-dependent manner (Fig. 5 E).

### IPO11 is required for CRC organoid growth

Activating mutations within Wnt pathway components are required during CRC initiation and progression. Consistent with a role for *IPO11* to sustain high levels of nuclear βcatenin activity, its expression is upregulated in CRC and rectal tumor samples compared with normal matched tissues (Fig. S2 A; TCGA mRNA expression dataset via OncoPrint, <https://www.oncoPrint.org/>; Cancer Genome Atlas Network, 2012). To confirm the functional importance of *IPO11* in this context, we observed a reduction of colony formation in *IPO11*<sup>-/-</sup> DLD-1 cells infected with gRNA targeting *IPO11* (Fig. 5 A). For all CRC cell lines containing an *APC* mutation, their growth dependency on *IPO11* positively correlated with *CTNNB1* dependency (*R* = 0.56, *P* = 0.016; Avana

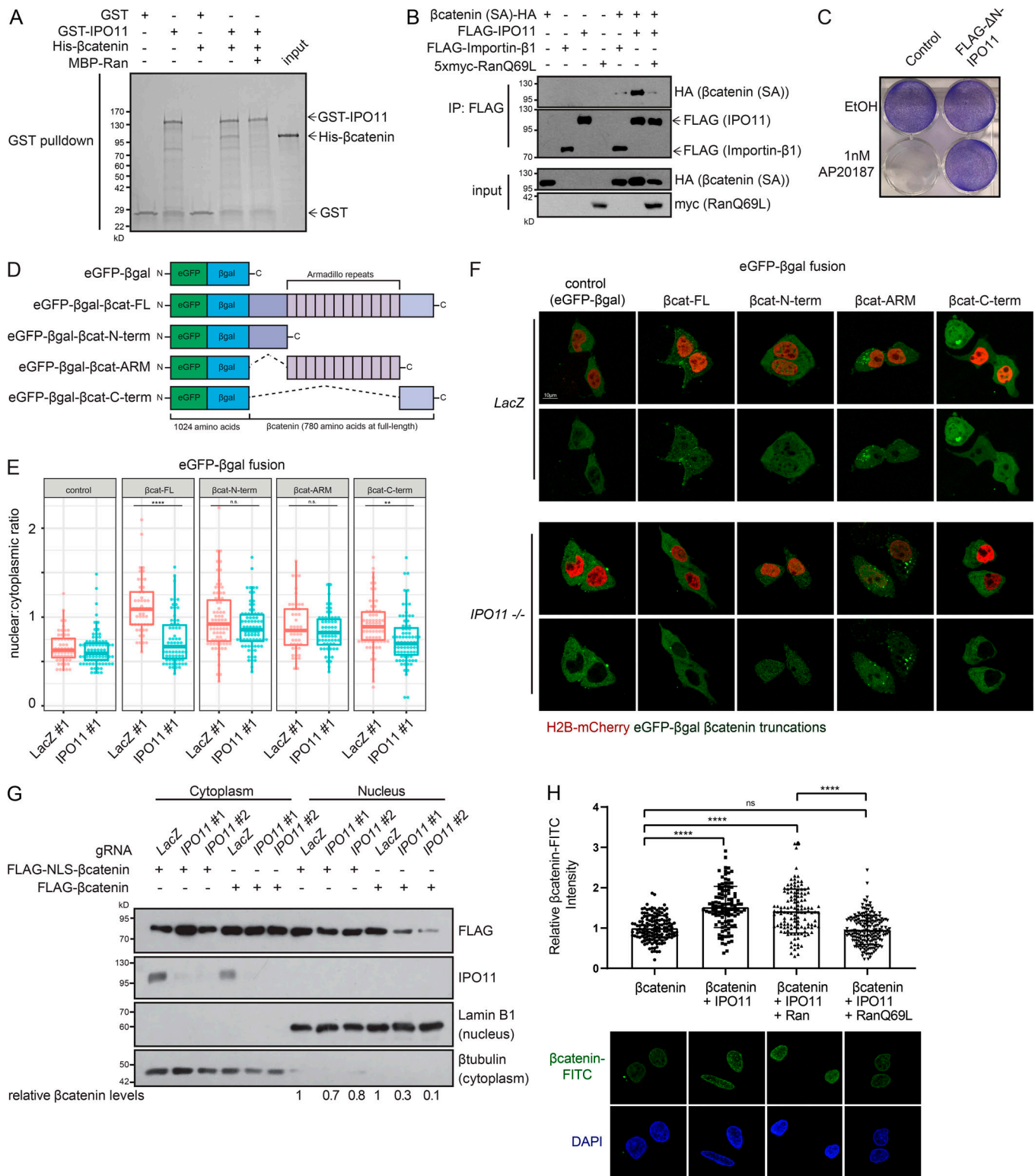


Figure 4. **IPO11 binds βcatenin to mediate its nuclear transport.** (A) GST-pull-down assay using purified IPO11 and βcatenin proteins. (B) HEK293T cells were transfected with the indicated expression plasmids, and lysates were subjected to coimmunoprecipitations followed by Western blot. (C) Crystal violet stain of DLD-1 βcatenin-DEADPOOL cells expressing FLAG-ΔN-IPO11 and treated with EtOH or 1 nM AP20187. (D) Schematic of eGFP-βgalactosidase-βcatenin fusion constructs. FL, full length. (E) Confocal microscopy-based quantification of nuclear to cytoplasmic eGFP intensity ratios for the indicated constructs expressed in control or *IPO11*<sup>-/-</sup> clones. Each point represents a single cell, with data collected over two independent experiments. *n* > 25 for each group. Two-way ANOVA Sidak's multiple comparison test. \*\*, *P* < 0.01; \*\*\*\*, *P* < 0.0001. (F) Representative images of E. (G) DLD-1 cells overexpressing FLAG-βcatenin or FLAG-NLS-βcatenin and *LacZ*, *IPO11* #1, and *IPO11* #2 gRNA were fractionated into cytoplasmic and nuclear compartments and immunoblotted for indicated proteins. (H) FITC-βcatenin nuclear import assay in semipermeabilized HeLa cells, imaged by confocal microscopy. Each point represents a single cell, pooled

from three independent experiments; representative images of each condition are presented. Ordinary one-way ANOVA with Sidak's multiple comparisons test, \*\*\*\*,  $P < 0.0001$ , mean  $\pm$  SD.  $\beta$ catenin alone,  $n = 148$ ;  $\beta$ catenin + Importin-11,  $n = 109$ ;  $\beta$ catenin + IPO11 + Ran,  $n = 128$ ;  $\beta$ catenin + IPO11 + RanQ69L,  $n = 191$ . ns, not significant.

CRISPR library via DepMap, <https://depmap.org>; Fig. S2 B; Meyers et al., 2017).

To support these findings, we next studied the requirement of *IPO11* for the growth of APC mutant CRC patient-derived three-dimensional organoids, which rely on cancer stem cell activity for growth (van de Wetering et al., 2015). KO of *IPO11* in the organoids led to reduced expression of the  $\beta$ catenin target gene *ASCL2*, suggesting that *IPO11* is required for  $\beta$ catenin activity in this context (Fig. 5 B). We then delivered gRNA in APC mutant CRC organoids and monitored their growth using a fluorescence-based imaging assay over multiple days (Fig. S3 C). Transduction of gRNAs targeting *CTNNB1* or *IPO11* reduced organoid growth only in Cas9-expressing organoids in which gene editing occurred (Fig. 5, C and D; and Fig. S3, D and E). We conclude that *IPO11* is required for growth of CRC cells.

In this study using the DEADPOOL system, we identified *IPO11* as a nuclear import factor for  $\beta$ catenin in CRC cells harboring APC mutations and high levels of constitutive ligand-independent signaling. Interestingly, *IPO11* was identified as a site of insertion for the mouse mammary tumor virus in mammary tumors (Theodorou et al., 2007), the same context in which Wnt proteins were discovered (Nusse et al., 1984). In bladder cancer, *IPO11* overexpression promotes migration and correlates with poor survival (Zhao et al., 2016, 2018). *IPO11* also regulates PTEN nuclear localization, where *IPO11* KO leads to tumor progression in the prostate (Chen et al., 2017). *IPO11* may therefore play context-dependent, sometimes opposite, roles in different cancers.

Our study reveals that *IPO11* is required in most CRC cell lines harboring APC mutations, whereas other tested CRC cell lines such as RKO and HCT116 show less *IPO11* dependency for  $\beta$ catenin localization and activation. This genotype-specific requirement reveals that context-dependent mechanisms for  $\beta$ catenin nuclear translocation exist. It is possible that these mechanisms coexist in cells and may be differentially engaged in zones of low or high Wnt activity. Passive diffusion of  $\beta$ catenin to the nucleus may be sufficient for ligand-dependent  $\beta$ catenin signaling and in the context of direct  $\beta$ catenin activating mutations; however, high  $\beta$ catenin signaling requirements in tissue stem cells or in APC mutant tumor cells may require additional  $\beta$ catenin nuclear import provided by an active IPO11-mediated process. It is important to further understand the biochemical nature of  $\beta$ catenin–IPO11 interaction in the context of truncated APC proteins. It is clear from our study that in most APC mutant contexts,  $\beta$ catenin relies on *IPO11* for nuclear import. This furthers our understanding of the molecular pathology of CRC.

The molecular mechanism underlying  $\beta$ catenin nuclear transport remains incompletely understood. Due to the homology of  $\beta$ catenin and Importin- $\alpha$  armadillo repeats, it has been suggested that  $\beta$ catenin mediates its own nuclear entry through the nuclear pore. In fact, overexpression of Importin- $\beta$ 1 reduces  $\beta$ catenin nuclear localization (Fagotto et al., 1998), which was

thought to be due to competition between Importin- $\beta$ 1 and  $\beta$ catenin for nuclear pore binding. Importin- $\beta$  proteins compete with one another for binding sites at the nuclear pore. However,  $\beta$ catenin overexpression does not block Importin- $\beta$ 1 nuclear localization (Yokoya et al., 1999), and  $\beta$ catenin fails to directly interact with nuclear pore proteins (Suh and Gumbiner, 2003), perhaps indicating that  $\beta$ catenin may be transported by an alternative Importin- $\beta$  other than Importin- $\beta$ 1. For example, overexpression of Importin- $\beta$ 1 reduces nuclear transport of the IPO11 cargo UBE2E3 (Plafker and Macara, 2000). In agreement with a Ran/Importin- $\beta$  mechanism,  $\beta$ catenin nuclear transport is temperature dependent and sensitive to depletion of ATP/GTP or the addition of nonhydrolyzable GTP analogues indicative of an active and energy-dependent process (Fagotto et al., 1998). We speculate that  $\beta$ catenin nuclear transport occurs in a similar manner to Importin- $\alpha$ , via parallel routes using both Ran/Importin- $\beta$ -dependent and -independent mechanisms that could be engaged through two different nuclear targeting signals previously identified in  $\beta$ catenin (Suh and Gumbiner, 2003; Fig. 5 E). Interestingly, our results indicate that whereas the isolated N-terminal, armadillo repeats and C-terminal domains of  $\beta$ catenin all localize to the nucleus of CRC cells, only the C-terminal domain does so in an IPO11-dependent manner. The separation of  $\beta$ catenin molecular determinants supporting passive diffusion versus IPO11-mediated nuclear localization offers an additional level of context-dependent regulation of signaling output but also may help explain, in part, the conflicting reports describing the mechanisms of  $\beta$ catenin nuclear transport.

## Materials and methods

### Plasmids

To make the pBAR-iCasp9 plasmid, the DNA fragment encoding for the FKBP-Casp9 (iCasp9) fusion protein was PCR amplified from pMSCV-F-del Casp9.IRES.GFP (#15567; Addgene) and ligated downstream of 12 $\times$  LEF-TCF elements (#12456) in a puromycin-resistant lentiviral plasmid. Lenti Cas9-2A-BsdR (#73310) and pLCKO (#73311) were obtained from Addgene. pH3 vector expressing (#12555; Addgene) IPO11 cDNA was a gift from Dr. Ian Macara (Vanderbilt University, Nashville, TN) that was used to clone IPO11 into a pcDNA3 backbone with Flag tag. HA- $\beta$ catenin SA cDNA was cloned into pIRESpuro-CBP-2 $\times$ TEV-StrepTag backbone (#17132; Addgene).  $\beta$ catenin, Ran, and IPO11 inserts were PCR amplified from cDNA and cloned into the respective backbones pET-28a (+), pMAL, and pGEX-GST. Flag-Lef1-VP16, Flag-IPO11, Flag- $\beta$ catenin, and Flag-NLS- $\beta$ catenin cDNA were PCR amplified and replaced the Cas9-BFP2 expression cassette in pAAVS1-tet-iCas9-BFP2 (#125519; Addgene) plasmid backbone. IPO11,  $\beta$ catenin, and Ran mutants were generated by PCR-based site-directed mutagenesis. eGFP- $\beta$ gal- $\beta$ catenin full-length and truncation plasmids were constructed by Gibson assembly and placed into pcDNA3 backbone.

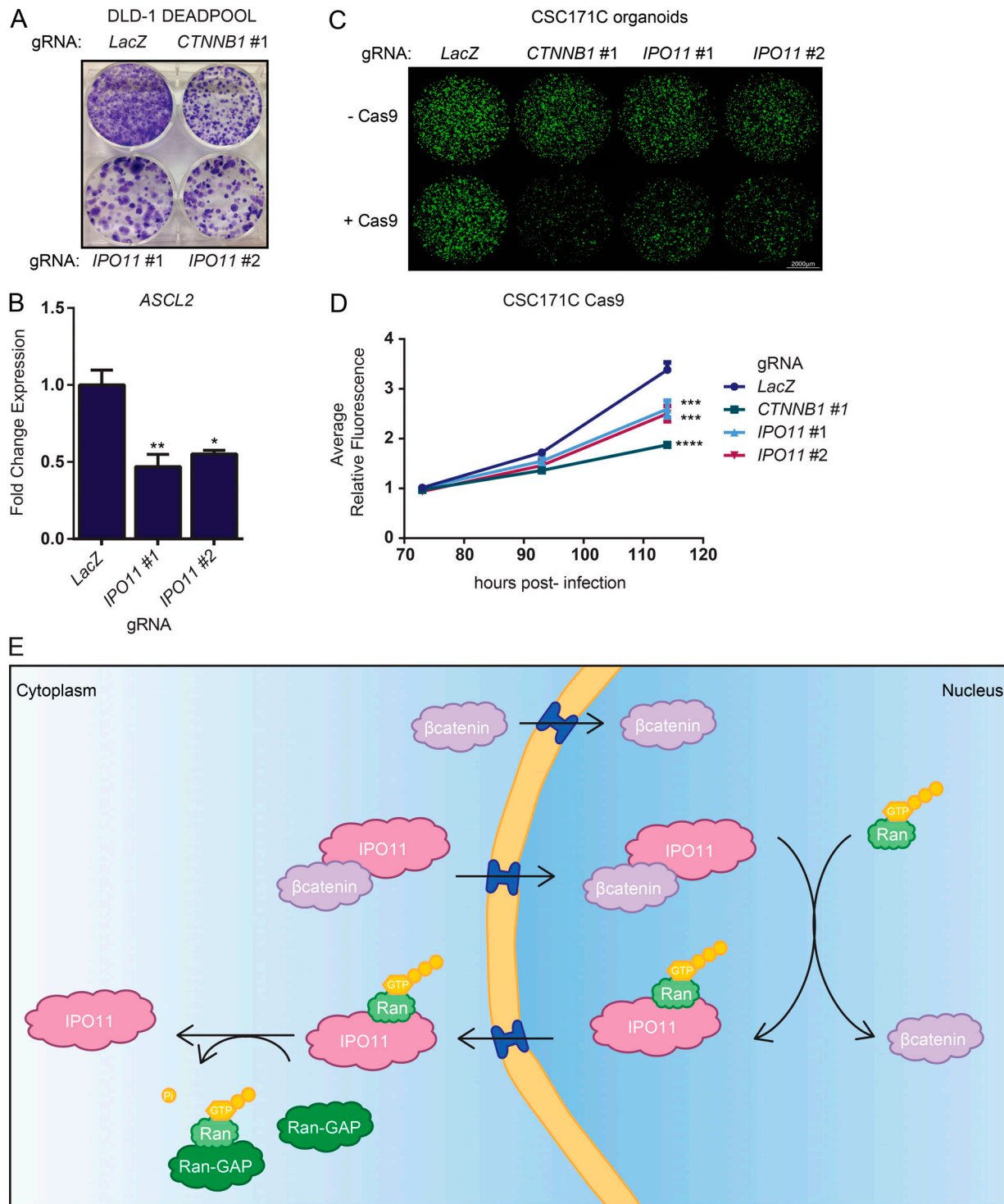


Figure 5. **IPO11 is required for CRC organoid growth.** (A) Crystal violet stain of colony formation of DLD-1  $\beta$ catenin-DEADPOOL cells transduced with *LacZ*, *IPO11* #1, and *IPO11* #2 gRNA. (B) RT-qPCR of *ASCL2* in CSC171C organoid line transduced with *LacZ*, *IPO11* #1, or *IPO11* #2 gRNA. Mean fold change  $\pm$  SD, representative of  $n = 3$  independent experiments. Statistical analysis was performed by one-way ANOVA Dunnett's test. \*,  $P \leq 0.05$ ; \*\*,  $P \leq 0.01$ . (C) Fluorescence images of CSC171C organoid line expressing Cas9 and gRNA for *LacZ*, *CTNNB1* #1, *IPO11* #1, or *IPO11* #2. (D) Points represent mean fold change  $\pm$  SD of fluorescence of C representative of  $n = 3$  independent experiments. Statistical analysis was performed by one-way ANOVA Dunnett's test. \*\*\*,  $P \leq 0.001$ ; \*\*\*\*,  $P \leq 0.0001$ . (E) Proposed model of  $\beta$ catenin nuclear translocation through direct binding of  $\beta$ catenin armadillo repeats and nuclear pore proteins via a Ran-independent mechanism. IPO11 directly binds  $\beta$ catenin in the cytoplasm to mediate  $\beta$ catenin nuclear import. In the nucleus, IPO11 binds to Ran-GTP, which leads to the dissociation of the cargo–importin- $\beta$  complex.  $\beta$ catenin accumulates in the nucleus.



### Development of the DLD-1 $\beta$ catenin-DEADPOOL cell line

DLD-1 cells were cotransduced with lenti Cas9-2A-BsdR (#73310; Addgene) and pBAR-iCasp9 and selected with 8  $\mu$ g/ml blasticidin and 100  $\mu$ g/ml hygromycin B. Single cells were isolated by serial dilution. Clonal lines were tested for response to B/B homodimerizer (AP20187 #635058; Takara Bio) and for Cas9 cutting efficiency.

### Cell culture

DLD-1, SW480, HeLa, and HEK293T cells were cultured in DMEM (4.5 g/liter D-glucose and L-glutamine; #11965; Thermo Fisher) with 10% fetal bovine serum (Thermo Fisher) and 5% penicillin/streptomycin (#15140-163; Thermo Fisher) at 37°C and 5% CO<sub>2</sub>. Cells were tested for mycoplasma with the MycoAlert mycoplasma detection kit (#LT07-118; Lonza).

### Viral production and transductions

Lentivirus was produced in HEK293T by calcium phosphate transfection of a 50% confluent 100-mm dish with 2  $\mu$ g vesicular stomatitis virus glycoprotein, 5  $\mu$ g psPAX2, and 5  $\mu$ g lentiviral vector. 24 h after transfection, medium was discarded and fresh medium was added. 48 h after transfection, virus-containing medium was collected and centrifuged at 1,000 *g* for 5 min and 0.45  $\mu$ m filtered. DLD-1 and SW480 cells were transduced with virus in the presence of 8  $\mu$ g/ml polybrene.

Virus intended for organoid cultures was concentrated with Lenti-X Concentrator (Takara) and incubated at 4°C overnight, centrifuged at 1,500 *g* for 45 min, and resuspended in 200  $\mu$ l of 1 $\times$  PBS. To transduce organoids with lentivirus, the protocol was adapted from Koo et al. (2012). In brief, pellets were resuspended in 200  $\mu$ l infection media (CRC media plus 10  $\mu$ M Y-27632, 10  $\mu$ M CIHR-99021, 10 mM nicotinamide, and 8  $\mu$ g/ml polybrene) and counted. 2.5  $\times$  10<sup>4</sup> cells were transferred to a round bottom tube, and 5  $\mu$ l of concentrated virus was added. Transductions were spinoculated for 1 h at 600 *g* at 32°C, then transferred to a 37°C 5% CO<sub>2</sub> incubator for 6 h. Transduced organoids were transferred to an Eppendorf tube and centrifuged at 500 *g* for 3 min at RT. Virus-containing supernatant was removed, and pellets were resuspended in 125  $\mu$ l of Matrigel (Corning). 25  $\mu$ l of Matrigel was seeded into four wells of a 48-well plate, and 250  $\mu$ l CRC media was added per well and changed every 2–3 d.

### Positive selection screen

The screen was adapted from Hart et al. (2015) using the TKOv1 CRISPR/Cas9 gRNA library. Briefly, the DLD-1  $\beta$ catenin-DEADPOOL cell line was infected with the TKOv1 library, which contains 91,320 gRNA targeting 17,232 human genes, with 8  $\mu$ g/ml polybrene at an MOI of 0.3 at 24 h after infection. Cells were subsequently treated with 3.5  $\mu$ g/ml of puromycin for 48 h. At 72 h, this population of gene-edited cells was split and cultured in the presence of EtOH (vehicle control) or 1 nM AP20187 and cultured in biological triplicate populations. EtOH-treated cells were passaged every 3 d and harvested on day 23. AP20187-treated cells were not passaged, and medium was changed every 3 d.

Genomic DNA was extracted using the QIAamp DNA Blood Maxi Kit (Qiagen) and precipitated using ethanol and sodium

chloride. gDNA samples were bar coded by PCR amplification using i5 and i7 adaptor primers for Illumina next-generation sequencing.

TruSeq adapter primers with i5 bar codes: 5'-AATGATACG GCGACCACCGAGATCTACACTATAGCCTACACTCTTTCCCTA CACGACGCTCTTCCGATCTTGTGGAAGGACGAGGTACCG-3'; 5'-AATGATACGGCGACCACCGAGATCTACACATAGAGGCACACT CTTTCCCTACACGACGCTCTTCCGATCTTGTGGAAGGACGAG GTACCG-3'; 5'-AATGATACGGCGACCACCGAGATCTACACCCTA TCCTACACTCTTTCCCTACACGACGCTCTTCCGATCTTGTGG AAGGACGAGGTACCG-3'; 5'-AATGATACGGCGACCACCGAGATC TACACGGCTCTGAACACTCTTCCCTACACGACGCTCTTCCG ATCTTGTGGAAGGACGAGGTACCG-3'

TruSeq adapter primers with i7 bar codes: 5'-CAAGCAGAA GACGGCATAACGATCGAGTAATGTGACTGGAGTTCAGACGT GTGCTCTTCCGATCTATTTAACTTGCTATTTCTAGCTCTAA AAC-3'; 5'-CAAGCAGAAGACGGCATAACGAGATTCTCCGGAGTGA CTGGAGTTCAGACGTGTGCTCTTCCGATCTATTTAACTTGCT ATTTCTAGCTCTAAAAC-3'; 5'-CAAGCAGAAGACGGCATAACGA GATAATGAGCGGTGACTGGAGTTCAGACGTGTGCTCTTCCGA TCTATTTAACTTGCTATTTCTAGCTCTAAAAC-3'; 5'-CAAGCA GAAGACGGCATAACGAGATGGAATCTCGTGACTGGAGTTCAGA CGTGTGCTCTTCCGATCTATTTAACTTGCTATTTCTAGCTC TAAAAC-3'.

Bar coded PCRs of T0, T23 EtOH (drop-out), and T23 AP20187 (positive selection) samples were sequenced with the Illumina HiSeq2500 with read depths of 500-, 200-, and 100-fold coverage, respectively.

The read counts for each gRNA were mapped to the gRNA library using MAGeCK (Li et al., 2014). Read counts for each gRNA were averaged across replicates for each condition. An enrichment score was calculated for each gRNA as the fold change of abundance in AP20187 normalized to EtOH-treated samples, then ranked in descending order. Genes with at least four gRNA with a Z score >3 were considered a hit in the screen.

### Individual gRNA construction and validation

pLCKO lentiviral vector (#73311; Addgene) was used for gRNA construction and was performed as previously described (Hart et al., 2015). Guide targeting sequences are the following: LacZ: 5'-CCGGTGCAGTATGAAGGCGG-3'; CTNNB1 #1: 5'-GAAAAGCGG CTGTTAGTCAC-3'; CTNNB1 #2: 5'-TCCCCTAATGTCCAGCGTT-3'; IPO11 #1: 5'-GATTGGATTGTCCCAGACAG-3'; and IPO11 #2: 5'-TCAGTTGAATAACTGGGAGC-3'. To confirm KO, genomic DNA was extracted using the PureLink Genomic DNA Mini Kit (Thermo Fisher), and PCR was performed using primers that flanked the cut site by ~600 base pairs. The resulting PCR product was purified using the PureLink PCR Purification Kit (Thermo Fisher) and sequenced by Sanger sequencing. Raw sequencing files were analyzed by the Tide web tool (Brinkman et al., 2014; <https://tide.nki.nl/>) to determine KO efficiency.

### Colony formation and fluorescence-based growth assays

DLD-1 DEADPOOL cells were transduced with gRNA as described above. After 24 h, transduced cells were selected for gRNA integration with 2  $\mu$ g/ml puromycin. 72 h after transduction, DLD-1 DEADPOOL cells containing gRNA were dissociated and

counted. 500 cells were seeded per condition and were cultured for 12 d with media changes every 2–3 d. The cells were fixed with 100% ice-cold MeOH for 20 min at  $-20^{\circ}\text{C}$ . Cells were stained with crystal violet solution (0.5% crystal violet and, 25% methanol) for 45 min at RT. Crystal violet solution was removed, and cells were washed five times with distilled  $\text{H}_2\text{O}$ .

Organoids were monitored by fluorescence imaging using the Cytation 5 Imaging Reader (BioTek) every 2–3 d. Multiple fluorescence images were stitched, and the intensity was quantified using Gen5 software.

### CRC organoid passaging

Embedded Matrigel culture of CRC organoids (obtained from Dr. Catherine O'Brien, University Health Network, Toronto, Ontario, Canada) was adapted from [Sato et al. \(2011\)](#). Briefly, media were removed, and 500  $\mu\text{l}$  of TrypLE Express (Thermo Fisher) was added per well. Matrigel fragments were scraped, transferred to an Eppendorf tube, and incubated at  $37^{\circ}\text{C}$  for 20 min. 2 ml of cold Advanced DMEM/F12 supplemented with Pen-Strep, 2 mM GlutaMAX, and 10 mM Hepes was added. Dissociated organoids were pelleted by centrifugation at 250  $g$  for 5 min at  $4^{\circ}\text{C}$ , and supernatant was removed. To keep organoids for passaging, 225  $\mu\text{l}$  of Matrigel was added per dissociated well. 25  $\mu\text{l}$  of Matrigel was seeded per well of a 48-well plate, and 250  $\mu\text{l}$  of organoids media (Advanced DMEM/F12, 2 mM GlutaMAX-I, 10 mM Hepes, 100 U/ml penicillin/streptomycin, B27, 1.25 mM N-acetyl-L-cysteine, 20 nM [Leu15]-Gastrin I, 50 ng/ml mouse EGF, 100 ng/ml mNoggin, and 0.5  $\mu\text{M}$  A83-01) was added per well and changed every 2–3 d.

### TOPflash reporter assay

Lentivirus containing the TOPflash  $\beta$ catenin-dependent Firefly luciferase and a normalizing Renilla luciferase were used to generate a stable DLD-1 TOPflash cell line with 100  $\mu\text{g}/\text{ml}$  hygromycin B selection. DLD-1 TOPflash cells were subsequently transduced with lentivirus containing gRNA. After 24 h, transduced cells were selected for gRNA integration with 2  $\mu\text{g}/\text{ml}$  puromycin. 7 d after gRNA infection, DLD-1 TOPflash cells were assayed for luciferase activity using the Dual-Luciferase Reporter Assay System (#E1910; Promega) using the Envision multilabel plate reader.

### RT-PCR and quantitative PCR (qPCR)

RNA was extracted from cells using TRIzol reagent (Thermo Fisher) per the manufacturer's protocol. 2  $\mu\text{g}$  of total RNA was DNase treated, and cDNA was synthesized in a 20- $\mu\text{l}$  reaction using the SuperScript II reverse transcription kit (Thermo Fisher). Real-time PCR reaction was made with 0.25  $\mu\text{l}$  of cDNA, primer mix, and SYBR Green according to the manufacturer's protocol (Thermo Fisher) and was performed on a 7900HT Fast Real-Time PCR system. mRNA levels were analyzed using Applied Biosystems software. Mean relative gene expression was normalized to housekeeping gene cyclophilin B by the  $\Delta\Delta\text{C}_t$  method ([Bookout et al., 2006](#)). The qPCR primer sequences are as follows: ASCL2 forward: 5'-CCCTCCAGCAGCTCAAGTTA-3', ASCL2 reverse: 5'-GGCACCAACACTTGAGATT-3', AXIN2 forward: 5'-CTCCCCACCTTGAATGAAGA-3', AXIN2 reverse: 5'-TGGCTGGTGCAAAGACATAG-3', KIAA1199 forward: 5'-AGA

GTGAGCCAGCTGATGGT-3', KIAA1199 reverse: 5'-ACTGTCTCG GCTACAGACCC-3', NKD1 forward: 5'-TGAGAAGATGGAGAG AGTGAGCGA-3', NKD1 reverse: 5'-GGTGACCTTGCCGTTGTT GTCAAA-3', TDGF1 forward: 5'-AAATGGCCATGATCCAAATC-3', TDGF1 reverse: 5'-CGATGCTAACGCCTCTTTTC-3', TNFRSF19 forward: 5'-GGAGTTGTCTAAGGAATGTGG-3', TNFRSF19 reverse: 5'-GCTGAACAATTTGCCTTCTG-3', cyclophilin B forward: 5'-GGAGATGGCACAGGAGGAA-3', cyclophilin B reverse: 5'-GCCCGTAGTGCTTCAGTTT-3', IPO11 forward: 5'-TCCTGT TTCAGGATCTTCCG-3', IPO11 reverse: 5'-CTTTCAGCTTTGGCT TTGCT-3', CTNNB1 forward: 5'-TACCTCCCAAGTCTGTATGA G-3', CTNNB1 reverse: 5'-TGAGCAGCATCAAACCTGTGTAG-3'.

### Nuclear fractionation

DLD-1 cells were harvested with trypsin and complete media, washed with ice-cold PBS, and immediately proceeded according to the manufacturer's protocol (NE-PER kit; Thermo Fisher). Fractions were quantified and 10  $\mu\text{g}$  of protein was loaded into each well.

### Coimmunoprecipitation

HEK293T cells were transfected with the indicated plasmids using PolyJet reagent according to the manufacturer's instructions (SigmaGen). 48 h after transfection, cells were harvested, washed with PBS, and lysed in 800  $\mu\text{l}$  of 0.1% TAP lysis buffer (10% glycerol, 50 mM Hepes-NaOH, pH 8, 150 mM NaCl, 2 mM EDTA, 0.1% NP-40, 2 mM DTT, 1 $\times$  protease inhibitor cocktail [Sigma-Aldrich], 10 mM NaF, 0.25 mM  $\text{Na}_3\text{VO}_3$  and  $\beta$ glycerophosphate, and 5 U benzonase) for 1 h at  $4^{\circ}\text{C}$ . Cell lysates were centrifuged at 16,000  $g$  for 15 min at  $4^{\circ}\text{C}$ . 80  $\mu\text{l}$  was kept for input, and the remaining lysate was incubated with prewashed Flag M2 beads (Sigma-Aldrich) for 3 h on rotator at  $4^{\circ}\text{C}$ . Beads were pelleted at 2,000  $g$  for 2 min, supernatant was removed, and beads were wash five times in 1 ml of lysis buffer. Laemmli loading buffer was added to the beads and boiled for 5 min at  $95^{\circ}\text{C}$ .

### Western blot antibodies

Primary antibodies were purchased from the respective vendors: rabbit anti-BCL9L (A303-152A; Bethyl), rabbit anti-IPO11 (A304-811A; Bethyl), rabbit ERK1/2 (#9102; Cell Signaling), rabbit  $\beta$ catenin for Western blot (#9587; Cell Signaling), rabbit Lamin B1 (#16048; Abcam), mouse anti- $\beta$ -tubulin clone TUB 2.1, rabbit anti-Flag (2368; Sigma-Aldrich), mouse anti-HA (clone 16B12; Covance), mouse myc antibody (#9E10; Abcam), and GST antibody (B-326, MA4-004). Secondary antibodies were conjugated to horseradish peroxidase (Jackson ImmunoResearch Laboratories Inc).

### Cellular $\beta$ catenin localization by confocal microscopy

SW480 cells were transduced with lentivirus, enabling expression of the indicated gRNA and selected with 2.5  $\mu\text{g}/\text{ml}$  puromycin. Cells were plated onto coverslips that were pretreated with 50  $\mu\text{g}/\text{ml}$  fibronectin for 24 h at  $4^{\circ}\text{C}$ . 72 h after seeding, cells were fixed in  $-20^{\circ}\text{C}$ , 100% MeOH overnight at  $-20^{\circ}\text{C}$ . Coverslips were washed two times with ice-cold PBS and permeabilized in 0.2% Triton X-100 in PBS with 10% normal donkey serum for 1 h. Coverslips were incubated in primary rabbit  $\beta$ catenin (#8480;

Cell Signaling) 1:50 antibodies in 0.2% Triton X-100 in PBS with 10% normal donkey serum at 4°C for 16 h. Coverslips were washed three times with PBS, then incubated with secondary anti-rabbit antibodies conjugated to Alexa Fluor 488 (Thermo Fisher) 1:500 in 0.2% Triton X-100 in PBS containing 10% normal donkey serum for 1 h in the dark at RT. Coverslips were washed five times for 5 min in PBS and mounted onto slides with Vectashield mounting medium (Vector Laboratories) containing DAPI. Images were acquired at room temperature on a laser scanning confocal microscope (LSM700; Carl Zeiss) at 12-bit with a Plan-Apochromat 63×/1.4 NA oil immersion objective using Zen software. To quantify  $\beta$ catenin localization, images were analyzed in ImageJ, the nucleus and whole cell were traced to two regions of interest, and intensity values for these areas were calculated. The relative nuclear intensity of  $\beta$ catenin was determined by measuring the mean fluorescence intensity of  $\beta$ catenin in the cytoplasm and nucleus of 50 cells per condition. The intensity and area of the cytoplasm was calculated by subtracting the intensity and area of the nucleus from the whole cell. Statistical analysis was done by one-way ANOVA Dunnett's test.

Various plasmids encoding fusion constructs between eGFP- $\beta$ galactosidase and either full-length  $\beta$ catenin or isolated  $\beta$ catenin domains were transfected along with a plasmid coding for H2B-mCherry (to label nuclei) in DLD-1 cells with lipofectamine2000 (Thermo Fisher) for 8 h followed by media change and overnight recovery. 24 h after transfection, cells were plated onto coverslips. After 24 h, cells were fixed in 2% paraformaldehyde at RT for 10 min. Coverslips were mounted onto slides with Vectashield. Images were acquired at room temperature on a laser scanning confocal microscope (LSM700; Carl Zeiss) at 12-bit with Plan-Apochromat 20×/1.4 NA oil immersion objective using Zen software. Nuclear and cytoplasmic fluorescence intensity was quantified using CellProfiler (Broad Institute; <https://cellprofiler.org>). Briefly, cells were identified using H2B-mCherry expression to localize the nuclei. Cell bodies were determined using the Distance-B method. Mean fluorescence intensity of the eGFP constructs was measured in each compartment: nucleus and cytoplasm (defined as nucleus minus cell body). Ratios of nuclear/cytoplasmic mean fluorescent intensity were calculated and normalized to LacZ-eGFP- $\beta$ gal condition, which was set to 1. Statistical analysis was done by two-way ANOVA Sidak's multiple comparison test.

#### GST-pulldown assay

BL21 bacteria were transformed with protein expression vectors pGEX-4T1 and pET-28B for GST and His-tagged proteins, respectively. Induction of protein expression was initiated at OD<sub>600</sub> of 0.8–1.0 with 0.5 mM IPTG as follows: GST, GST-Importin- $\beta$ 1, GST-IPO11 4 h at RT, His- $\beta$ catenin 3 h at 37°C. Bacterial pellets were lysed with GST lysis buffer (50 mM Tris, pH 7.4, 150 mM NaCl, 1% Triton X-100, 10% glycerol, 1 mM EDTA, 1 mM PMSF, 0.2 mg/ml lysozyme, and 1 mM T-Cep) or His lysis buffer (20 mM sodium phosphate, pH 7.4, 500 mM NaCl, with 1 mM T-Cep, and 1 mM PMSF) and sonicated. Lysates were cleared by centrifugation at 16,000 g for 30 min at 4°C and incubated with glutathione-sepharose 4B (GE Healthcare) or Hislink (Promega) resin. Bound proteins were washed with GST

lysis buffer or His wash buffer (His lysis buffer with 60 mM imidazole), and His- $\beta$ catenin was eluted from beads with 500 mM imidazole in lysis buffer. GST beads were resuspended in 500  $\mu$ l of binding buffer (50 mM Tris, pH 7.4, 150 mM NaCl, 0.1% NP-40, 1 mM EDTA, 20% glycerol, and protease inhibitor cocktail [Sigma-Aldrich]), incubated with purified His- $\beta$ catenin protein for 2 h at 4°C, washed with binding buffer, and eluted with 4× Laemmli buffer.

#### Nuclear import assay

The protocol was adapted from a previous study (Cassany and Gerace, 2009). GST-purified  $\beta$ catenin was conjugated to FITC using a commercial kit (Thermo Fisher). Dye ratio was estimated to be 1.2 molecules per molecule of protein. pcDNA3.1-FLAG-IPO11 was transfected in 293T cells and 48 h after transfection was purified using FLAG-M2 beads (Sigma-Aldrich). IPO11 was eluted using 100  $\mu$ g/ml FLAG peptide (Sigma-Aldrich). Both  $\beta$ catenin and IPO11 were concentrated using Amicon 30-kD filters (Millipore). For the import assay, HeLa cells were grown in eight-well chamber slides. The following day, cells were permeabilized in 0.004% digitonin (Thermo Fisher), the cytoplasm was washed out, and the indicated components (360  $\mu$ M FITC- $\beta$ catenin, 2  $\mu$ M Ran or RanQ69L, and 600 nM IPO11) in transport buffer (20 mM Hepes, pH 7.4, 110 mM potassium acetate, 2 mM magnesium acetate, 1 mM EGTA, 2 mM DTT, 1 mM PMSF, and protease inhibitor [Sigma-Aldrich]) were added. Cells were incubated for 30 min at 37°C. Following transport washout, cells were fixed in 4% paraformaldehyde and coverslips were mounted using Vectashield containing DAPI (Vector Laboratories). Images were acquired at room temperature on a laser scanning confocal microscope (LSM700; Carl Zeiss) at 12-bit with Plan-Apochromat 20×/1.4 for quantification and 40×/1.4 for representation of NA oil immersion objective using Zen software. Nuclear intensity was quantified using CellProfiler, nuclei were identified using DAPI stain, and intensity was measured in the FITC channel. Nuclear intensity of each replicate was normalized to the  $\beta$ catenin-alone condition and expressed at relative FITC intensity.

#### Gene essentiality analysis

Essentiality data for *IPO11* in colon/colorectal cell lines were retrieved from PICKLES (Lenoir et al., 2018) using the 18Q4 Avana library dataset. The APC mutation status of cell lines was retrieved from COSMIC using the DepMap online tool (Meyers et al., 2017; <https://depmap.org/portal>) and binned according to their mutation status (wild type or mutant).

#### Statistical analysis

Statistical analysis was performed using Graphpad Prism Software. Data are represented as mean  $\pm$  SD. Statistical analysis of multiple samples was performed by one-way ANOVA Dunnett's test unless stated otherwise. In cases with uneven sample sizes, the Mann-Whitney *U* test was used.

#### Online supplemental material

Fig. S1 shows that *IPO11* KO does not affect  $\beta$ catenin transcription. Fig. S2 shows *IPO11* expression and gene dependency in CRCs.

Fig. S3 shows purification and conjugation of His- $\beta$ -catenin and FLAG-IPO11 and patient-derived CRC organoid growth assay.

## Acknowledgments

We thank all of the members of the Angers laboratory, past and present, who provided insightful comments for the project. We especially thank Nishani Rajakulendran for editing the manuscript. We are also grateful to Dr. Catherine O'Brien and Dr. Jennifer Haynes (University Health Network, Toronto, Ontario, Canada) for providing the CRC organoids.

This work was supported by grants from the Canadian Institutes of Health Research (364969) to S. Angers and (342551) to J. Moffat as well as by the Canadian Cancer Society (705045) to S. Angers. M. Mis and S. O'Brien were supported by Ontario Graduate Scholarships and Centre for Pharmaceutical Oncology Scholarships. T. Hart was supported by National Institutes of Health grants P30CA016672 and R35GM130119 and Cancer Prevention and Research Institute of Texas grant RR160032.

The authors declare no competing financial interests.

Author contributions: S. Angers and M. Mis conceptualized the study and designed the experiments. M. Mis performed the experiments. T. Hart and Z. Steinhart analyzed the screen data. S. Angers and M. Mis wrote the original manuscript. M. Mis, S. O'Brien, S. Lin, and Z. Steinhart performed revision experiments and revised the manuscript. S. Angers and J. Moffat supervised the study. S. Angers acquired funding for research.

Submitted: 4 March 2019

Revised: 9 August 2019

Accepted: 7 November 2019

## References

- Angers, S., and R.T. Moon. 2009. Proximal events in Wnt signal transduction. *Nat. Rev. Mol. Cell Biol.* 10:468–477. <https://doi.org/10.1038/nrm2717>
- Behrens, J., B.A. Jerchow, M. Würtele, J. Grimm, C. Asbrand, R. Wirtz, M. Kühl, D. Wedlich, and W. Birchmeier. 1998. Functional interaction of an axin homolog, conductin, with  $\beta$ -catenin, APC, and GSK3 $\beta$ . *Science*. 280: 596–599. <https://doi.org/10.1126/science.280.5363.596>
- Bookout, A.L., C.L. Cummins, D.J. Mangelsdorf, J.M. Pesola, and M.F. Kramer. 2006. High-throughput real-time quantitative reverse transcription PCR. *Curr. Protoc. Mol. Biol.* 73:15.8.1–15.8.28.
- Brinkman, E.K., T. Chen, M. Amendola, and B. van Steensel. 2014. Easy quantitative assessment of genome editing by sequence trace decomposition. *Nucleic Acids Res.* 42:e168. <https://doi.org/10.1093/nar/gku936>
- Cadigan, K.M., and M.L. Waterman. 2012. TCF/LEFs and Wnt signaling in the nucleus. *Cold Spring Harb. Perspect. Biol.* 4:a007906. <https://doi.org/10.1101/cshperspect.a007906>
- Cancer Genome Atlas Network. 2012. Comprehensive molecular characterization of human colon and rectal cancer. *Nature*. 487:330–337. <https://doi.org/10.1038/nature11252>
- Cassany, A., and L. Gerace. 2009. Reconstitution of nuclear import in permeabilized cells. *Methods Mol. Biol.* 464:181–205. [https://doi.org/10.1007/978-1-60327-461-6\\_11](https://doi.org/10.1007/978-1-60327-461-6_11)
- Chen, M., D.G. Nowak, N. Narula, B. Robinson, K. Watrud, A. Ambrico, T.M. Herzka, M.E. Zeeman, M. Minderer, W. Zheng, et al. 2017. The nuclear transport receptor Importin-II is a tumor suppressor that maintains PTEN protein. *J. Cell Biol.* 216:641–656. <https://doi.org/10.1083/jcb.201604025>
- Di Stasi, A., S.-K. Tey, G. Dotti, Y. Fujita, A. Kennedy-Nasser, C. Martinez, K. Straathof, E. Liu, A.G. Durett, B. Grilley, et al. 2011. Inducible apoptosis as a safety switch for adoptive cell therapy. *N. Engl. J. Med.* 365: 1673–1683. <https://doi.org/10.1056/NEJMoal106152>
- Dominguez, I., K. Itoh, and S.Y. Sokol. 1995. Role of glycogen synthase kinase 3 beta as a negative regulator of dorsoventral axis formation in *Xenopus* embryos. *Proc. Natl. Acad. Sci. USA*. 92:8498–8502. <https://doi.org/10.1073/pnas.92.18.8498>
- Dow, L.E., K.P. O'Rourke, J. Simon, D.F. Tschaharganeh, J.H. van Es, H. Clevers, and S.W. Lowe. 2015. Apc Restoration Promotes Cellular Differentiation and Reestablishes Crypt Homeostasis in Colorectal Cancer. *Cell*. 161:1539–1552. <https://doi.org/10.1016/j.cell.2015.05.033>
- Fagotto, F., U. Glück, and B.M. Gumbiner. 1998. Nuclear localization signal-independent and importin/karyopherin-independent nuclear import of  $\beta$ -catenin. *Curr. Biol.* 8:181–190. [https://doi.org/10.1016/S0960-9822\(98\)70082-X](https://doi.org/10.1016/S0960-9822(98)70082-X)
- Fearon, E.R. 2011. Molecular genetics of colorectal cancer. *Annu. Rev. Pathol.* 6: 479–507. <https://doi.org/10.1146/annurev-pathol-011110-130235>
- Fearon, E.R., and B. Vogelstein. 1990. A genetic model for colorectal tumorigenesis. *Cell*. 61:759–767. [https://doi.org/10.1016/0092-8674\(90\)90186-I](https://doi.org/10.1016/0092-8674(90)90186-I)
- Hart, T., M. Chandrashekar, M. Aregger, Z. Steinhart, K.R. Brown, G. MacLeod, M. Mis, M. Zimmermann, A. Fradet-Turcotte, S. Sun, et al. 2015. High-Resolution CRISPR Screens Reveal Fitness Genes and Genotype-Specific Cancer Liabilities. *Cell*. 163:1515–1526. <https://doi.org/10.1016/j.cell.2015.11.015>
- Henderson, B.R. 2000. Nuclear-cytoplasmic shuttling of APC regulates  $\beta$ -catenin subcellular localization and turnover. *Nat. Cell Biol.* 2:653–660. <https://doi.org/10.1038/35023605>
- Jamieson, C., M. Sharma, and B.R. Henderson. 2014. Targeting the  $\beta$ -catenin nuclear transport pathway in cancer. *Semin. Cancer Biol.* 27:20–29. <https://doi.org/10.1016/j.semcancer.2014.04.012>
- Kimura, M., and N. Imamoto. 2014. Biological significance of the importin- $\beta$  family-dependent nucleocytoplasmic transport pathways. *Traffic*. 15: 727–748. <https://doi.org/10.1111/tra.12174>
- Kimura, M., Y. Morinaka, K. Imai, S. Kose, P. Horton, and N. Imamoto. 2017. Extensive cargo identification reveals distinct biological roles of the 12 importin pathways. *eLife*. 6:e21184. <https://doi.org/10.7554/eLife.21184>
- Koo, B.-K., D.E. Stange, T. Sato, W. Karthaus, H.F. Farin, M. Huch, J.H. van Es, and H. Clevers. 2012. Controlled gene expression in primary Lgr5 organoid cultures. *Nat. Methods*. 9:81–83. <https://doi.org/10.1038/nmeth.1802>
- Kramps, T., O. Peter, E. Brunner, D. Nellen, B. Froesch, S. Chatterjee, M. Murone, S. Züllig, and K. Basler. 2002. Wnt/wingless signaling requires BCL9/legless-mediated recruitment of pygopus to the nuclear  $\beta$ -catenin-TCF complex. *Cell*. 109:47–60. [https://doi.org/10.1016/S0092-8674\(02\)00679-7](https://doi.org/10.1016/S0092-8674(02)00679-7)
- Krieghoff, E., J. Behrens, and B. Mayr. 2006. Nucleo-cytoplasmic distribution of  $\beta$ -catenin is regulated by retention. *J. Cell Sci.* 119:1453–1463. <https://doi.org/10.1242/jcs.02864>
- Lenoir, W.F., T.L. Lim, and T. Hart. 2018. PICKLES: the database of pooled in-vitro CRISPR knockout library essentiality screens. *Nucleic Acids Res.* 46(D1):D776–D780. <https://doi.org/10.1093/nar/gkx993>
- Li, W., H. Xu, T. Xiao, L. Cong, M.I. Love, F. Zhang, R.A. Irizarry, J.S. Liu, M. Brown, and X.S. Liu. 2014. MAGeCK enables robust identification of essential genes from genome-scale CRISPR/Cas9 knockout screens. *Genome Biol.* 15:554. <https://doi.org/10.1186/s13059-014-0554-4>
- Mackmull, M.-T., B. Klaus, I. Heinze, M. Chokkalingam, A. Beyer, R.B. Russell, A. Ori, and M. Beck. 2017. Landscape of nuclear transport receptor cargo specificity. *Mol. Syst. Biol.* 13:962. <https://doi.org/10.15252/msb.20177608>
- Major, M.B., B.S. Roberts, J.D. Berndt, S. Marine, J. Anastas, N. Chung, M. Ferrer, X. Yi, C.L. Stoick-Cooper, P.D. von Haller, et al. 2008. New regulators of Wnt/ $\beta$ -catenin signaling revealed by integrative molecular screening. *Sci. Signal.* 1:ra12. <https://doi.org/10.1126/scisignal.2000037>
- Marikawa, Y., and R.P. Elinson. 1998.  $\beta$ -TrCP is a negative regulator of Wnt/ $\beta$ -catenin signaling pathway and dorsal axis formation in *Xenopus* embryos. *Mech. Dev.* 77:75–80. [https://doi.org/10.1016/S0925-4773\(98\)00134-8](https://doi.org/10.1016/S0925-4773(98)00134-8)
- Meyers, R.M., J.G. Bryan, J.M. McFarland, B.A. Weir, A.E. Sizemore, H. Xu, N.V. Dharia, P.G. Montgomery, G.S. Cowley, S. Pantel, et al. 2017. Computational correction of copy number effect improves specificity of CRISPR-Cas9 essentiality screens in cancer cells. *Nat. Genet.* 49: 1779–1784. <https://doi.org/10.1038/ng.3984>
- Morin, P.J., A.B. Sparks, V. Korinek, N. Barker, H. Clevers, B. Vogelstein, and K.W. Kinzler. 1997. Activation of  $\beta$ -catenin-Tcf signaling in colon cancer by mutations in  $\beta$ -catenin or APC. *Science*. 275:1787–1790. <https://doi.org/10.1126/science.275.5307.1787>

- Nusse, R., A. van Ooyen, D. Cox, Y.K. Fung, and H. Varmus. 1984. Mode of proviral activation of a putative mammary oncogene (int-1) on mouse chromosome 15. *Nature*. 307:131–136. <https://doi.org/10.1038/307131a0>
- Peters, J.M., R.M. McKay, J.P. McKay, and J.M. Graff. 1999. Casein kinase I transduces Wnt signals. *Nature*. 401:345–350. <https://doi.org/10.1038/43830>
- Plafker, S.M., and I.G. Macara. 2000. Importin-11, a nuclear import receptor for the ubiquitin-conjugating enzyme, UbcM2. *EMBO J.* 19:5502–5513. <https://doi.org/10.1093/emboj/19.20.5502>
- Rexach, M., and G. Blobel. 1995. Protein import into nuclei: association and dissociation reactions involving transport substrate, transport factors, and nucleoporins. *Cell*. 83:683–692. [https://doi.org/10.1016/0092-8674\(95\)90181-7](https://doi.org/10.1016/0092-8674(95)90181-7)
- Rosin-Arbesfeld, R., A. Cliffe, T. Brabletz, and M. Bienz. 2003. Nuclear export of the APC tumour suppressor controls beta-catenin function in transcription. *EMBO J.* 22:1101–1113. <https://doi.org/10.1093/emboj/cdg105>
- Sato, T., D.E. Stange, M. Ferrante, R.G.J. Vries, J.H. Van Es, S. Van den Brink, W.J. Van Houdt, A. Pronk, J. Van Gorp, P.D. Siersema, et al. 2011. Long-term expansion of epithelial organoids from human colon, adenoma, adenocarcinoma, and Barrett's epithelium. *Gastroenterology*. 141:1762–1772. <https://doi.org/10.1053/j.gastro.2011.07.050>
- Scholer-Dahirel, A., M.R. Schlabach, A. Loo, L. Bagdasarian, R. Meyer, R. Guo, S. Woolfenden, K.K. Yu, J. Markovits, K. Killary, et al. 2011. Maintenance of adenomatous polyposis coli (APC)-mutant colorectal cancer is dependent on Wnt/beta-catenin signaling. *Proc. Natl. Acad. Sci. USA*. 108:17135–17140. <https://doi.org/10.1073/pnas.1104182108>
- Shalem, O., N.E. Sanjana, E. Hartenian, X. Shi, D.A. Scott, T. Mikkelsen, D. Heckl, B.L. Ebert, D.E. Root, J.G. Doench, et al. 2014. Genome-scale CRISPR-Cas9 knockout screening in human cells. *Science*. 343:84–87. <https://doi.org/10.1126/science.1247005>
- Steinhart, Z., and S. Angers. 2018. Wnt signaling in development and tissue homeostasis. *Development*. 145:dev146589. <https://doi.org/10.1242/dev.146589>
- Straathof, K.C., M.A. Pulè, P. Yotnda, G. Dotti, E.F. Vanin, M.K. Brenner, H.E. Heslop, D.M. Spencer, and C.M. Rooney. 2005. An inducible caspase 9 safety switch for T-cell therapy. *Blood*. 105:4247–4254. <https://doi.org/10.1182/blood-2004-11-4564>
- Suh, E.-K., and B.M. Gumbiner. 2003. Translocation of beta-catenin into the nucleus independent of interactions with FG-rich nucleoporins. *Exp. Cell Res.* 290:447–456. [https://doi.org/10.1016/S0014-4827\(03\)00370-7](https://doi.org/10.1016/S0014-4827(03)00370-7)
- Theodorou, V., M.A. Kimm, M. Boer, L. Wessels, W. Theelen, J. Jonkers, and J. Hilkens. 2007. MMTV insertional mutagenesis identifies genes, gene families and pathways involved in mammary cancer. *Nat. Genet.* 39:759–769. <https://doi.org/10.1038/ng2034>
- Townsend, F.M., A. Cliffe, and M. Bienz. 2004. Pygopus and Legless target Armadillo/beta-catenin to the nucleus to enable its transcriptional co-activator function. *Nat. Cell Biol.* 6:626–633. <https://doi.org/10.1038/ncb1141>
- van de Wetering, M., H.E. Francies, J.M. Francis, G. Bounova, F. Iorio, A. Pronk, W. van Houdt, J. van Gorp, A. Taylor-Weiner, L. Kester, et al. 2015. Prospective derivation of a living organoid biobank of colorectal cancer patients. *Cell*. 161:933–945. <https://doi.org/10.1016/j.cell.2015.03.053>
- Wodarz, A., and R. Nusse. 1998. Mechanisms of Wnt signaling in development. *Annu. Rev. Cell Dev. Biol.* 14:59–88. <https://doi.org/10.1146/annurev.cellbio.14.1.59>
- Yokoya, F., N. Imamoto, T. Tachibana, and Y. Yoneda. 1999.  $\beta$ -catenin can be transported into the nucleus in a Ran-unassisted manner. *Mol. Biol. Cell*. 10:1119–1131. <https://doi.org/10.1091/mbc.10.4.1119>
- Zhao, J., W. Xu, M. He, Z. Zhang, S. Zeng, C. Ma, Y. Sun, and C. Xu. 2016. Whole-exome sequencing of muscle-invasive bladder cancer identifies recurrent copy number variation in IPO11 and prognostic significance of importin-11 overexpression on poor survival. *Oncotarget*. 7:75648–75658. <https://doi.org/10.18632/oncotarget.12315>
- Zhao, J., L. Shi, S. Zeng, C. Ma, W. Xu, Z. Zhang, Q. Liu, P. Zhang, Y. Sun, and C. Xu. 2018. Importin-11 overexpression promotes the migration, invasion, and progression of bladder cancer associated with the deregulation of CDKN1A and THBS1. *Urol. Oncol.* 36:311.e1–311.e13. <https://doi.org/10.1016/j.urolonc.2018.03.001>